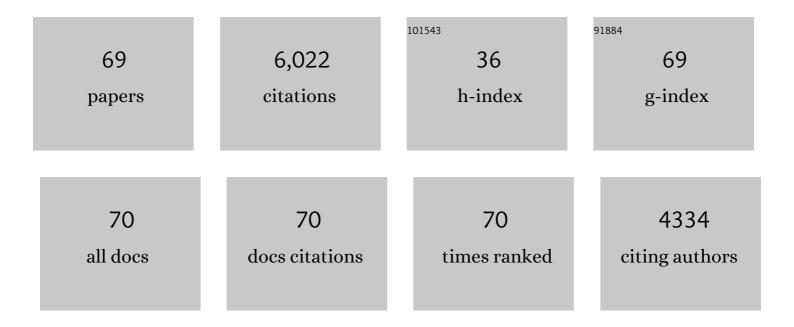
William D Carlson

List of Publications by Year in descending order

Source: https://exaly.com/author-pdf/3810325/publications.pdf Version: 2024-02-01



#	Article	IF	CITATIONS
1	Acquisition, optimization and interpretation of X-ray computed tomographic imagery: applications to the geosciences. Computers and Geosciences, 2001, 27, 381-400.	4.2	1,172
2	Variability of apatite fission-track annealing kinetics; III, Extrapolation to geological time scales. American Mineralogist, 1999, 84, 1235-1255.	1.9	656
3	Variability of apatite fission-track annealing kinetics; II, Crystallographic orientation effects. American Mineralogist, 1999, 84, 1224-1234.	1.9	355
4	Scales of disequilibrium and rates of equilibration during metamorphism. American Mineralogist, 2002, 87, 185-204.	1.9	219
5	Rates of Fe, Mg, Mn, and Ca diffusion in garnet. American Mineralogist, 2006, 91, 1-11.	1.9	204
6	The significance of intergranular diffusion to the mechanisms and kinetics of porphyroblast crystallization. Contributions To Mineralogy and Petrology, 1989, 103, 1-24.	3.1	194
7	Disequilibrium for Ca during growth of pelitic garnet. Journal of Metamorphic Geology, 1997, 15, 421-438.	3.4	150
8	Optical Determination of Topotactic Aragonite-Calcite Growth Kinetics: Metamorphic Implications. Journal of Geology, 1981, 89, 615-638.	1.4	145
9	Rates and mechanism of Y, REE, and Cr diffusion in garnet. American Mineralogist, 2012, 97, 1598-1618.	1.9	144
10	Plagioclase-chain networks in slowly cooled basaltic magma. American Mineralogist, 1999, 84, 1819-1829.	1.9	139
11	Three-dimensional quantitative textural analysis of metamorphic rocks using high-resolution computed X-ray tomography: Part II. Application to natural samples. Journal of Metamorphic Geology, 1997, 15, 45-57.	3.4	133
12	Trace element zoning as a record of chemical disequilibrium during garnet growth. Geology, 1999, 27, 555.	4.4	123
13	Mechanisms of Porphyroblast Crystallization: Results from High-Resolution Computed X-ray Tomography. Science, 1992, 257, 1236-1239.	12.6	120
14	Controls on the nucleation and growth of porphyroblasts: Kinetics from natural textures and numerical models. Geological Journal, 1995, 30, 207-225.	1.3	102
15	The origin of olivine-plagioclase coronas in metagabbros from the Adirondack Mountains, New York. Journal of Metamorphic Geology, 1990, 8, 697-717.	3.4	100
16	The Portales Valley meteorite breccia: evidence for impact-induced melting and metamorphism of an ordinary chondrite. Geochimica Et Cosmochimica Acta, 2001, 65, 323-342.	3.9	93
17	Three-dimensional imaging of earth and planetary materials. Earth and Planetary Science Letters, 2006, 249, 133-147.	4.4	90
18	Topology of syntectonic melt-flow networks in the deep crust; inferences from three-dimensional images of leucosome geometry in migmatites. American Mineralogist, 1999, 84, 1793-1818.	1.9	89

#	Article	IF	CITATIONS
19	Timing of Colorado Plateau uplift: Initial constraints from vesicular basalt-derived paleoelevations. Geology, 2002, 30, 807.	4.4	88
20	Diamonds and Their Mineral Inclusions, and What They Tell Us: A Detailed "Pull-Apart―of a Diamondiferous Eclogite. International Geology Review, 2000, 42, 959-983.	2.1	82
21	Origins of yttrium and rare earth element distributions in metamorphic garnet. Journal of Metamorphic Geology, 2013, 31, 663-689.	3.4	81
22	Implications of garnet resorption for the Lu-Hf garnet geochronometer: an example from the contact aureole of the Makhavinekh Lake Pluton, Labrador. Journal of Metamorphic Geology, 2011, 29, 901-916.	3.4	80
23	Competitive diffusion-controlled growth of porphyroblasts. Mineralogical Magazine, 1991, 55, 317-330.	1.4	76
24	An overgrowth model to explain multiple, dispersed high-Mn regions in the cores of garnet porphyroblasts. American Mineralogist, 2003, 88, 131-141.	1.9	71
25	Sizes and Masses of Chondrules and Metal–Troilite Grains in Ordinary Chondrites: Possible Implications for Nebular Sorting. Icarus, 1999, 141, 96-106.	2.5	69
26	Analysis of Vesicular Basalts and Lava Emplacement Processes for Application as a Paleobarometer/Paleoaltimeter. Journal of Geology, 2002, 110, 671-685.	1.4	67
27	Nature of diamonds in Yakutian eclogites: views from eclogite tomography and mineral inclusions in diamonds. Lithos, 2004, 77, 333-348.	1.4	67
28	Metamorphism as Garnet Sees It: The Kinetics of Nucleation and Growth, Equilibration, and Diffusional Relaxation. Elements, 2013, 9, 439-445.	0.5	66
29	Beyond the equilibrium paradigm: How consideration of kinetics enhances metamorphic interpretation. American Mineralogist, 2015, 100, 1659-1667.	1.9	63
30	Mesoproterozoic plate tectonics: A collisional model for the Grenville-aged orogenic belt in the Llano uplift, central Texas. Geology, 2008, 36, 55.	4.4	60
31	Fluid evolution and transport during metamorphism: evidence from the Llano Uplift, Texas. Contributions To Mineralogy and Petrology, 1986, 92, 518-529.	3.1	59
32	Porphyroblast crystallization: linking processes, kinetics, and microstructures. International Geology Review, 2011, 53, 406-445.	2.1	47
33	Metasomatic origin of diamonds in the world's largest diamondiferous eclogite. Lithos, 2009, 112, 1014-1024.	1.4	45
34	Prograde, peak, and retrograde P-T paths from aluminium in orthopyroxene: High-temperature contact metamorphism in the aureole of the Makhavinekh Lake Pluton, Nain Plutonic Suite, Labrador. Journal of Metamorphic Geology, 2003, 21, 405-423.	3.4	44
35	Graves Nunataks 95209: A snapshot of metal segregation and core formation. Geochimica Et Cosmochimica Acta, 2006, 70, 516-531.	3.9	43
36	Contrasting response of monazite and zircon to a high-T thermal overprint. Lithos, 2006, 88, 135-149.	1.4	40

#	Article	IF	CITATIONS
37	Monazite and xenotime petrogenesis in the contact aureole of the Makhavinekh Lake Pluton, northern Labrador. Contributions To Mineralogy and Petrology, 2005, 148, 524-541.	3.1	35
38	Effects of matrix grain size on the kinetics of intergranular diffusion. Journal of Metamorphic Geology, 2004, 22, 733-742.	3.4	34
39	Intracrystalline redistribution of Pb in zircon during high-temperature contact metamorphism. Chemical Geology, 2005, 217, 1-28.	3.3	34
40	Improved methods for quantitative analysis of three-dimensional porphyroblastic textures. , 2005, 1, 42.		31
41	Aragonite-Calcite Nucleation Kinetics: An Application and Extension of Avrami Transformation Theory. Journal of Geology, 1983, 91, 57-71.	1.4	30
42	DIFFUSION-CONTROLLED SYNKINEMATIC GROWTH OF GARNET FROM A HETEROGENEOUS PRECURSOR AT PASSO DEL SOLE, SWITZERLAND. Canadian Mineralogist, 2005, 43, 157-182.	1.0	30
43	Statistical analysis of bubble and crystal size distributions: Application to Colorado Plateau basalts. Journal of Volcanology and Geothermal Research, 2007, 164, 112-126.	2.1	30
44	Incorporation of Y and REEs in aluminosilicate garnet: Energetics from atomistic simulation. American Mineralogist, 2014, 99, 1022-1034.	1.9	30
45	Origin and mechanical significance of honeycomb garnet in high-pressure metasedimentary rocks from the Tauern Window, Eastern Alps. Journal of Metamorphic Geology, 2007, 25, 565-583.	3.4	29
46	High-pressure metamorphism during the Llano orogeny inferred from Proterozoic eclogite remnants. Geology, 1988, 16, 391.	4.4	28
47	Ti resetting in quartz during dynamic recrystallization: Mechanisms and significance. American Mineralogist, 2014, 99, 2025-2030.	1.9	28
48	Microstructural, chemical and textural records during growth of snowball garnet. Journal of Metamorphic Geology, 2009, 27, 423-437.	3.4	27
49	Magnitudes of departures from equilibrium during regional metamorphism of porphyroblastic rocks. Journal of Metamorphic Geology, 2013, 31, 981-1002.	3.4	27
50	Numerical simulation of diffusionâ€controlled nucleation and growth of porphyroblasts. Journal of Metamorphic Geology, 2012, 30, 489-512.	3.4	25
51	Crystallization kinetics during regional metamorphism of porphyroblastic rocks. Journal of Metamorphic Geology, 2013, 31, 963-979.	3.4	24
52	Controls on metamorphic equilibration: the importance of intergranular solubilities mediated by fluid composition. Journal of Metamorphic Geology, 2015, 33, 123-146.	3.4	24
53	High-Pressure Metamorphism in the Texas Grenville Orogen: Mesoproterozoic Subduction of the Southern Laurentian Continental Margin. International Geology Review, 2007, 49, 99-119.	2.1	22
54	Rates of Li diffusion in garnet: Coupled transport of Li and Y+REEs. American Mineralogist, 2014, 99, 1676-1682.	1.9	22

#	Article	IF	CITATIONS
55	Late thermal evolution of Proterozoic rocks in the northeastern Llano Uplift, central Texas. Precambrian Research, 1999, 94, 49-72.	2.7	21
56	Reversed pyroxene phase equilibria in CaO-MgO-SiO2 from 925ïį½ to 1,175ïį½ C at one atmosphere pressure. Contributions To Mineralogy and Petrology, 1986, 92, 218-224.	3.1	17
57	Evidence against the stability of orthoenstatite above â^¼1005°C at atmospheric pressure in CaOâ€MgOâ€6iO ₂ . Geophysical Research Letters, 1985, 12, 409-411.	4.0	13
58	Strain rates at high temporal resolution from curved inclusion trails in garnet, Passo del Sole, Central Swiss Alps. Journal of Metamorphic Geology, 2013, 31, 243-262.	3.4	13
59	Grenville-age orogeny in the Llano Uplift of central Texas: Deformation and metamorphism of the Rough Ridge Formation. Bulletin of the Geological Society of America, 1989, 101, 876-883.	3.3	11
60	Extent of chondrule melting: Evaluation of experimental textures, nominal grain size, and convolution index. Meteoritics and Planetary Science, 2006, 41, 1059-1071.	1.6	10
61	Variations in rates of nucleation and growth of biotite porphyroblasts. Journal of Metamorphic Geology, 2006, 24, 763-777.	3.4	10
62	Petrologic Constraints on the Tectonic Evolution of the Llano Uplift. Proceedings of the International Conferences on Basement Tectonics, 1998, , 3-27.	0.1	8
63	Nondestructive evaluation of cavitation in an Al–Mg material deformed under creep conditions. Journal of Materials Research, 2000, 15, 76-84.	2.6	7
64	Epitaxial nucleation of garnet on biotite in the polymetamorphic metapelites surrounding the Vedrette di Ries intrusion (Italian Eastern Alps). European Journal of Mineralogy, 2015, 27, 5-18.	1.3	6
65	Multicomponent diffusion in aluminosilicate garnet: coupling effects due to charge compensation. International Geology Review, 2017, 59, 526-540.	2.1	6
66	Vanadium pentoxide as a high-temperature solvent for phase equilibrium studies in CaO-MgO-Al2O3-SiO2. Contributions To Mineralogy and Petrology, 1986, 92, 89-92.	3.1	3
67	Laser Raman microspectrometry of metamorphic quartz: A simple method for comparison of metamorphic pressures–Corrigendum. American Mineralogist, 2009, 94, 1291-1292.	1.9	3
68	Evaluation of a combined HRXCT/EBSD method for detecting epitaxial nucleation of garnet porphyroblasts. European Journal of Mineralogy, 2015, 27, 19-29.	1.3	3
69	Correlation factors for impurity diffusion on the sublattice of dodecahedral sites in garnet. Physics and Chemistry of Minerals, 2016, 43, 363-369.	0.8	1